

# Gravity-Powered Chemical Dose Controller for Sustainable, Municipal-Scale Drinking Water Treatment

Karen A. Swetland\*, Monroe L. Weber-Shirk<sup>†</sup> and Leonard W. Lion<sup>‡</sup>

## Abstract

Accurate chemical dosing in water treatment plants is imperative to ensure optimal efficiency of flocculation and disinfection. Design algorithms, calibration techniques, and standardized components are presented for a linear flow orifice meter (LFOM) and a linear chemical dose controller (LCDC). These coupled systems allow water treatment plant operators to easily and reliably set and maintain the desired doses of coagulant and disinfectant. The combined system adjusts the chemical flow rate automatically in response to changes in plant flow rate to maintain the target chemical dose. The LFOM maintains a linear relationship between height of water in the entrance tank and plant flow rate. A lever and float are used to create a direct relationship between the plant flow and chemical flow produced by the LCDC. A linear relationship between head loss and chemical flow in the LCDC is created by using the major head loss through a small diameter tube to control the chemical flow rate. Experimental tests are described that minimize minor losses and verify performance of the LCDC.

Subject headings: coagulation; flow control; flow measurement; municipal water; water treatment plants; control systems;

## Introduction

The accurate application of coagulant prior to rapid mix and the addition of disinfectant after filtration are essential to the production of safe, clean drinking water at municipal drinking water treatment facilities. Reliable and easily maintained chemical dosing systems are vital. Many municipal water treatment plant chemical dosing systems rely on electronic supervisory control and data acquisition (SCADA) dose control systems to regulate the addition of coagulant and disinfectant. SCADA control systems are complex and require multiple interdependent technology platforms including sensors, signal convertors, microprocessors,

---

\*Graduate student, School of Civil and Environmental Engineering, Hollister Hall, Cornell University, Ithaca, NY, 14853. Email: kas444@cornell.edu

<sup>†</sup>Senior lecturer / Research Associate, School of Civil and Environmental Engineering, Hollister Hall, Cornell University, Ithaca, NY, 14853 (corresponding author). Email: mw24@cornell.edu. Phone: 1 607 216 8445 Fax: 1 607 255 9004

<sup>‡</sup>Professor, School of Civil and Environmental Engineering, Hollister Hall, Cornell University, Ithaca, NY, 14853. Email: LWL3@cornell.edu

28 software, and variable speed pumps. SCADA-type technology platforms also often rely on  
29 proprietary components and require a high level of technical expertise in each platform for  
30 maintenance. As a consequence, SCADA dose control systems have many failure modes and  
31 a significant number of the ensuing failures can require either replacement of specialized parts  
32 or the presence of highly trained technicians. These systems may be appropriate in facilities  
33 that have ready access to replacement part suppliers and that have financial capacity to pay  
34 the high labor costs for maintenance and technical support. However, SCADA-based water  
35 treatment plants perform poorly where replacement parts are not easily obtained and are  
36 commonly abandoned in developing countries when critical components malfunction. Sim-  
37 plified chemical dosing systems underpinned by sophisticated designs have been created to  
38 promote sustainable operation and are presented in this paper.

### 39 *Design Constraints for Sustainability:*

40 The AguaClara Program at Cornell University has developed a set of design guidelines for  
41 the creation of sustainable water treatment technologies. These guidelines embody lessons  
42 learned from years of experience inventing new technologies and taking them to full scale  
43 implementation through the program's collaboration with Agua Para el Pueblo in Honduras.  
44 The AguaClara drinking water treatment plants represent a new paradigm with a focus on  
45 the interaction between the plant operator and the technology. The design guidelines used by  
46 the AguaClara program that directly influenced the creation of the chemical dose controller  
47 and flow measurement systems described here are as follow:

48 To be operator-friendly, economical, and resilient, municipal scale water treatment plant  
49 designs must...

- 50 • be optimized for low cost and high performance.
- 51 • be easy to construct using low-precision construction techniques.
- 52 • minimize use of moving parts.
- 53 • operate without electricity.
- 54 • be observable (no sealed reactors) so that the plant operator can receive appropriate  
55 feedback for performance of every step of the treatment process.
- 56 • operate without requiring numerical calculations.
- 57 • use chemical dosages that can be set directly by the operator.
- 58 • be maintainable by one person.

59 A common method of chemical dosing employed in developing countries is the drip feed  
60 system consisting of a chemical stock tank with a small orifice through which the chemical  
61 exits (WHO, 2011). These systems are unable to maintain a constant chemical feed rate  
62 since the chemical flow rate decreases as the liquid level in the chemical stock tank drops. A

63 floating bowl chlorinator is an example of a dosing system that addresses this problem and  
 64 maintains a constant flow rate by maintaining a constant driving head even as the liquid level  
 65 varies (Brikke and Bredero, 2003). However, this system and other stand alone chemical flow  
 66 controllers regulates the chemical flow rate rather than the chemical dose. Chemical flow  
 67 controllers require the operator to adjust the chemical flow rate when the plant flow rate  
 68 is changed and that adjustment is generally by trial and error. Chemical flow controllers  
 69 represent a level of simplicity that functions reliably but delivers less than what a water  
 70 treatment plant operator needs.

71 A different solution to the chemical dosing challenge can be obtained given the goals of  
 72 maximizing reliability, reducing costs, minimizing the use of components that are not avail-  
 73 able in the local hardware store, and empowering plant operators to maintain and repair the  
 74 dosing systems. Reliability can be maximized by reducing the number of components and  
 75 technology platforms. The number of technology platforms can be substantially reduced by  
 76 using analog kinematics that connect linearized flow measurement to linearized flow control  
 77 and completely eliminating the dependence on software, digital electronics, chemical pumps,  
 78 and electricity. Dose controllers that use a minimum number of components can be described  
 79 as simplicity on the other side of complexity. This type of dosing system requires sophis-  
 80 ticated design methods (complexity), however the resulting device is simple to understand  
 81 and easy to operate and maintain.

82 The AguaClara plant dose controller that has been implemented in several water treat-  
 83 ment plants by the AguaClara program of Agua Para el Pueblo in Honduras has a minimum  
 84 number of parts and can be easily repaired if a problem is discovered. The dosing system  
 85 has two main components: (1) a linear flow orifice meter (LFOM) that creates a linear vari-  
 86 ation between water height and plant flow and (2) a linear chemical dose controller (LCDC)  
 87 that provides a chemical flow that is directly proportional to plant flow rate. The design,  
 88 construction, and testing of these components are described below.

## 89 Theory and Design

### 90 Linear Flow Orifice Meter

91 The Sutro Weir developed by Victor Sutro in 1915 mimics a Stout weir and creates a linear  
 92 relationship between height of water and flow rate. A Stout weir is a theoretical flow control  
 93 device in which weir width is proportional to  $1/\sqrt{\text{water height}}$ . It is not physically possible  
 94 to fabricate such a device because the base would be infinitely wide. The Sutro weir, shown  
 95 in Figure 1 serves as a practical alternative to the Stout weir. The width of the base,  $W$ ,  
 96 and upper portion of Sutro weir,  $y$ , as a function of height can be calculated by Equations  
 97 1 and 2, respectively.

$$W = \frac{Q_{Max}}{H_{Sutro}^{3/2} C_D \sqrt{3g} \Pi_{Sutro}} \quad (1)$$

$$y = \frac{W}{2} \left[ 1 - \frac{2}{\pi} \arctan \left( \sqrt{\frac{z_{Sutro}}{s}} \right) \right] \quad (2)$$

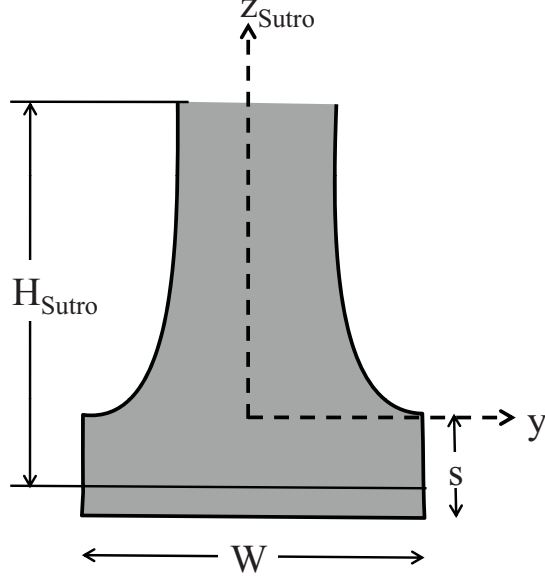


Figure 1: Diagram of the Sutro weir

98 where  $W$  is the width of the rectangular base of the weir,  $Q_{Max}$  is the maximum flow  
 99 through the weir,  $H_{Sutro}$  is the total height of the weir measured from  $s/3$  above the bottom  
 100 of the rectangular weir,  $\Pi_{Sutro}$  is  $(2s/3)/H_{Sutro}$ ,  $C_D$  is a discharge coefficient,  $g$  is acceleration  
 101 due to gravity,  $z_{Sutro}$  is the vertical distance from the start of a curved section, and  $s$  is the  
 102 height of the rectangular base (Thandaveswara, 2012). The theoretical flow through the  
 103 Sutro weir,  $Q_{Sutro}$ , is described by Equation 3.

$$Q_{Sutro} = \frac{W}{2} \left( 2C_D \sqrt{2gsh} \right) \quad (3)$$

104 where  $h$  is the vertical height of water measured from  $s/3$  above the bottom of the rectangular  
 105 weir. Equation 3 is only valid when the height of water is above the rectangular portion  
 106 ( $h \geq 2s/3$ ).

107 Accurate fabrication of a Sutro weir is somewhat difficult and the Sutro weir has the  
 108 unfortunate property that the flow rate does not actually go to zero when  $h = 0$  because  
 109 the rectangular opening extends below the datum used for the linear relationship between  
 110 flow and height. These two disadvantages were addressed in the linear flow orifice meter  
 111 (LFOM) described in this paper. The LFOM approximates a Sutro weir using a vertical  
 112 PVC pipe with a pattern of identically sized holes that create a linear relationship between  
 113 water height and plant flow. The simple construction of the LFOM eliminates the need for  
 114 skilled labor and uses readily available materials and tools. The LFOM is typically located  
 115 in the entrance tank of the water treatment plant where water flows through the orifices  
 116 created by the holes in the vertical pipe on its way to rapid mix and flocculation. The flow  
 117 through each individual hole,  $Q_{Orifice}$ , is described by the vertical orifice equation (Equation  
 118 4). With correct placement of multiple holes, the overall flow can be rendered linear with  
 119 respect to height of water in the tank, justifying the designation as a Linear Flow Orifice  
 120 Meter (LFOM).

$$Q_{Orifice} = \Pi_{vc} \sqrt{2g} \int_0^{\min(D_{Orifice}, h)} D_{Orifice} \sin \left[ \arccos \left( \frac{2z}{D_{Orifice}} \right) \right] \sqrt{h-z} dz \quad (4)$$

121 where  $\Pi_{vc}$  is the cross-sectional area of the constricted flow divided by the area of the orifice  
 122 caused by the vena contracta for the orifice ( $\Pi_{vc} = 0.62$  for all cases),  $D_{Orifice}$  is the diameter  
 123 of the orifice,  $z$  is integrated from 0 to the minimum of the orifice diameter and height of  
 124 water ( $\min(D_{Orifice}, h)$ ), and  $h$  is the height of water above the bottom of the orifice (Franz  
 125 and Melching, 1997).

126 There are many potential approaches to the design of an orifice based linear flow meter.  
 127 The design presented here uses a vertical PVC pipe of appropriate diameter (based on plant  
 128 flow as described below), a single standard sized drill bit, a minimum number of holes, and a  
 129 target water level change that is appropriate to drive the dose controller. The algorithm that  
 130 creates the LFOM hole pattern compensates for the fact that the orifices are all the same  
 131 size and that there must be an integer number of rows of orifices and an integer number of  
 132 orifices in each row. The algorithm steps are as follow:

- 133 1. calculate the minimum diameter of the vertical pipe required to maintain supercritical  
 134 flow at the bottom of the LFOM.
- 135 2. calculate the row spacing to allow use of a large orifice size to minimize the number of  
 136 holes drilled.
- 137 3. calculate the orifice size constrained to be a standard drill bit size, smaller than the  
 138 row spacing.
- 139 4. calculate the number of orifices in each row starting at the bottom row.

140 The LFOM pipe must be large enough in diameter to ensure that the pressure inside the  
 141 LFOM at the bottom row of orifices is atmospheric and that the flow inside the LFOM is  
 142 supercritical. Supercritical flow in the LFOM ensures that it is unaffected by changes in  
 143 downstream water levels. Each orifice jet accelerates downward due to gravity and the jets  
 144 collide and exchange momentum. The very bottom of the LFOM has the highest flow rate  
 145 inside the pipe and this flow velocity must be high enough so that the LFOM pipe is not  
 146 completely full of water. The average vertical velocity of water at the very bottom inside  
 147 the LFOM can be obtained by applying free fall acceleration to each orifice jet and then  
 148 applying conservation of momentum in the vertical direction to obtain the average vertical  
 149 velocity. This analysis can be simplified substantially by using the Stout weir equation to  
 150 approximate the vertical velocity of the free falling water at the bottom of the LFOM weir  
 151 (Equation 5). The velocity of water exiting the Stout weir as a function of height when the  
 152 weir is fully submerged,  $h = H_{Stout}$ , is:

$$V_{Stout} = \sqrt{2g(H_{Stout} - z)} \quad (5)$$

153 The Stout weir equation for the width of the weir as a function of height,  $z$ , is:

$$W_{Stout} = \frac{2Q}{H_{Stout} \Pi_{vc} \pi \sqrt{2gz}} \quad (6)$$

154 where  $Q$  is the flow through the Stout weir when the constant water depth is  $H_{Stout}$  and  $\Pi_{vc}$   
 155 is the vena contracta coefficient, 0.62.

156 The average velocity of the falling water at the bottom of the Stout weir,  $V_{Stout_{z=0}}$ , can  
 157 be obtained by integrating over the depth of the weir to obtain the total momentum in the  
 158 vertical direction of the falling water when it arrives at the bottom of weir. The average  
 159 velocity at the bottom of the weir is then obtained by dividing the total momentum by the  
 160 total mass flux. The water enters the Stout weir with no vertical velocity. The vertical  
 161 velocity obtained by the time it reaches the bottom of the weir is given by  $\sqrt{2gz}$ .

$$V_{Stout_{z=0}} = \frac{\int_0^{H_{Stout}} \rho_{Water} V_{Stout} W_{Stout} \Pi_{vc} \sqrt{2gz} dz}{\rho_{Water} Q} \quad (7)$$

162 where  $\rho_{Water}$  is the density of water. Substituting equations 6 and 5 into Equation 7 and  
 163 simplifying gives:

$$V_{Stout_{z=0}} = \frac{4\sqrt{2gH_{Stout}}}{3\pi} \quad (8)$$

164 Although the total effective width vs height for an LFOM is slightly different than for the  
 165 Stout weir, Equation 8 can be used to estimate the vertical velocity of water at the bottom  
 166 of the LFOM. For an LFOM with  $H_{LFOM} = 20 \text{ cm}$ ,  $V_{Stout_{z=0}} = 0.841 \text{ m/s}$ . A wide range of  
 167 plant flow rates can be accommodated by a maximum height of  $20 \text{ cm}$  through the LFOM.  
 168 The cross-sectional area and diameter of the pipe, can then be found by Equations 9 and 10  
 169 respectively.

$$A_{LFOM} = \Pi_{Safety} \frac{Q}{V_{Stout_{z=0}}} \quad (9)$$

$$D_{LFOM} = 2\sqrt{\frac{A_{LFOM}}{\pi}} \quad (10)$$

170 where  $\Pi_{Safety}$  is a safety factor (1.5 used here) that ensures that the velocity at the bottom  
 171 of the LFOM pipe is more than adequate to ensure that the pipe is not full of water and  
 172 thus the pressure inside the LFOM is atmospheric. In the design algorithm, the LFOM pipe  
 173 inner diameter is rounded up to the nearest available pipe size.

174 Before the surface area of the LFOM can be distributed as a series of orifices, the vertical  
 175 center-to-center spacing of the rows of orifices,  $B_{Row}$  must be found. The design calculation  
 176 is initialized with two orifices in the top row of orifices (Equation 12); however, this number  
 177 may subsequently be changed as the algorithm progresses. The width of the top of the Stout  
 178 weir,  $W_{Stout_{z=H_{LFOM}}}$ , is used to approximate the average width of the weir corresponding to  
 179 the top row of orifices in the LFOM.

$$B_{RowMax} W_{Stout_{z=H_{LFOM}}} = 2 \frac{\pi D_{Orifice}^2}{4} \quad (11)$$

180 where  $B_{RowMax}$  is the maximum row height and  $D_{Orifice}$  is the diameter of the orifices in  
 181 the LFOM. Since both  $B_{RowMax}$  and  $D_{Orifice}$  are unknown, the orifice diameter,  $D_{Orifice}$ ,  
 182 is assumed to equal to the maximum row height allowing Equation 11 to be solved for the  
 183 maximum row height.

$$B_{RowMax} = \frac{2}{\pi} W_{Stout_{z=H_{LFOM}}} \quad (12)$$

184 The number of rows of orifices,  $N_{Rows}$ , is obtained by dividing the user specified maximum  
 185 height of the LFOM,  $H_{LFOM}$ , by  $B_{RowMax}$  and rounding up to the nearest integer with the  
 186 additional constraint that the total number of rows be between 4 and 10. Linearity between  
 187 water height and flow is poor when the water level is in the first row of orifices and Equation  
 188 4 applies. AguaClara water treatment plants use a minimum of 4 rows to provide a linear  
 189 response down to 25% of the maximum flow rate. Accuracy increases with the addition of  
 190 more rows and is quite high with 10 rows. There is no advantage to having more than 10  
 191 rows as more rows require drilling more holes but does not greatly improve accuracy.

192 The next design step is to calculate the orifice diameter. The top row of orifices will  
 193 contain at least one hole. Thus, the orifice area,  $A_{TopOrifice}$ , in the top row must be equal to  
 194 or less than the theoretical stout weir area corresponding to the top row (Equation 13). An  
 195 estimate of the area of the top row of orifices is obtained by integrating Equation 6.

$$\frac{\pi}{4} D_{OrificeMax}^2 = A_{TopOrifice} = \int_{H_{LFOM}-B_{Row}}^{H_{LFOM}} \frac{2Q}{H_{LFOM} \Pi_{vc} \pi \sqrt{2gz}} dz \quad (13)$$

196 where  $D_{OrificeMax}$  is the maximum orifice diameter,  $Q$  is the maximum plant rate,  $g$  is  
 197 acceleration due to gravity, and  $z$  is the LFOM height over which the equation is integrated.

198 The diameter of the orifices,  $D_{Orifice}$ , is constrained to be less than  $D_{OrificeMax}$ , and  
 199 also less than  $B_{Row}$  and rounded down to the nearest available drill bit size. All orifices in  
 200 the LFOM design will have this diameter to simplify fabrication. The maximum number of  
 201 orifices that will physically fit along the circumference of the LFOM pipe,  $N_{MaxOrificeperRow}$ ,  
 202 is another constraint (Equation 14) that is important for high flow rates. The minimum  
 203 spacing between orifices needed to maintain the structural integrity of the pipe,  $S_{MinSpacing}$ ,  
 204 is 5 mm.

$$N_{MaxOrificeperRow} = \frac{\pi D_{LFOM}}{D_{Orifice} + S_{MinSpacing}} \quad (14)$$

205 If the number of orifices required in the bottom row exceeds the maximum number of  
 206 orifices that fit in the circumference of the pipe then the design must be modified by either  
 207 increasing the height of the LFOM or by further increasing the diameter of the pipe.

208 The final step in designing the LFOM is to calculate the number of orifices in each row.  
 209 Because the flow rate through the LFOM is linearly proportional to the height of water in  
 210 the entrance tank, the expected flow rate through the LFOM,  $Q_{Nsubmerged}$ , when  $N_{Submerged}$   
 211 rows of orifices are submerged is equal to Equation 15.

$$Q_{Nsubmerged} = Q \frac{B_{Row} N_{Submerged}}{H_{LFOM}} \quad (15)$$

212 With an orifice diameter and an expected flow rate per row, the number of orifices per  
 213 row,  $N_{Orifices}$ , can be calculated for each row using Equation 16 starting at the bottom and  
 214 incrementing  $N_{Submerged}$ . The vertical orifice equation (Equation 4) is used to find the flow  
 215 through a single orifice,  $Q_{Orifice}$ . As the number of orifices in each row is calculated, the

Table 1: Summary of Design Specifications for a Linear Flow Orifice Meter (LFOM)

Input	Value	Output	Value
$Q_{Plant}$	10 L/s	$B_{Row}$	2 cm
<i>Drill Bits</i>	<i>US Standard</i>	$D_{LFOM}$	15.2 cm (6 in)
$H_{LFOM}$	20 cm	$D_{Orifice}$	1.9 cm (0.75 in)
$S_{MinSpacing}$	5 mm	$Error_{Max}$	0.34%

216 flow provided by the lower rows,  $Q_{N-1submerged}$ , is subtracted from the total expected flow,  
 217  $Q_{Nsubmerged}$ , based on their depth of submergence to obtain flow required through the row  
 218 of orifices being calculated. The required flow through the row being calculated is divided  
 219 by the flow per orifice,  $Q_{Orifice}$  from (Equation 4), and the result is rounded to the nearest  
 220 integer to obtain the number of orifices required. Once the LFOM pattern of orifices is  
 221 drilled, the flow rate that corresponds to the water height at each row of the LFOM pattern  
 222 can be written on the LFOM pipe itself, allowing the operator to read the flow rate directly,  
 223 avoiding the need for mathematical calculations.

$$N_{Orifices} = \frac{Q_{Nsubmerged} - Q_{N-1submerged}}{Q_{Orifice}} \quad (16)$$

224 Table 1 provides an example of the input and output design parameters for an LFOM for a  
 225 plant with a maximum design flow of 10 L/s. Figure 2 shows equivalent designs for the Sutro  
 226 weir and LFOM with their respective flow profiles. Flow through the LFOM as a function  
 227 of depth remains linear when orifices are partially full. Custom designs for LFOMs may be  
 228 obtained at no charge from the AguaClara Design Tool ([aguaclara.cornell.edu/design](http://aguaclara.cornell.edu/design)).

## 229 Linear Chemical Dose Controller

230 With the linear relationship between height of water in the entrance tank and plant flow  
 231 rate provided by the LFOM, the linear chemical dose controller (LCDC) utilizes a float in  
 232 the entrance tank and a lever to connect the chemical flow rate to plant flow rate. When  
 233 the plant flow rate increases, the water level in the entrance tank rises proportionally, and  
 234 the float and lever arm rise as illustrated in Figure 3. A stock tank provides a reservoir  
 235 of the chemical solution (coagulant or disinfectant) and is connected to a constant head  
 236 tank. The constant head tank is regulated by a float valve which keeps the chemical depth  
 237 constant. A small diameter tube, referred to here as the dosing tube, leads from the stock  
 238 tank to a connector tube and then to a vertical drop tube that delivers the chemical to the  
 239 chemical injection point. The chemical flow rate is controlled by the length of the dosing  
 240 tube and the elevation head driving the flow - the vertical distance between the chemical  
 241 surface in the constant head tank and the outlet of the connector tube where it reaches the  
 242 vertical drop tube. The vertical drop tube is connected to the lever arm via a slider. The  
 243 plant operator sets the slider at the desired coagulant dose based upon characteristics of  
 244 the influent water. A locking mechanism holds the slider in place on the lever arm. The  
 245 float attached to the lever arm changes elevation in response to plant flow rate changes, thus  
 246 changing the elevation of the dosing tube outlet, and maintaining a constant chemical dose.



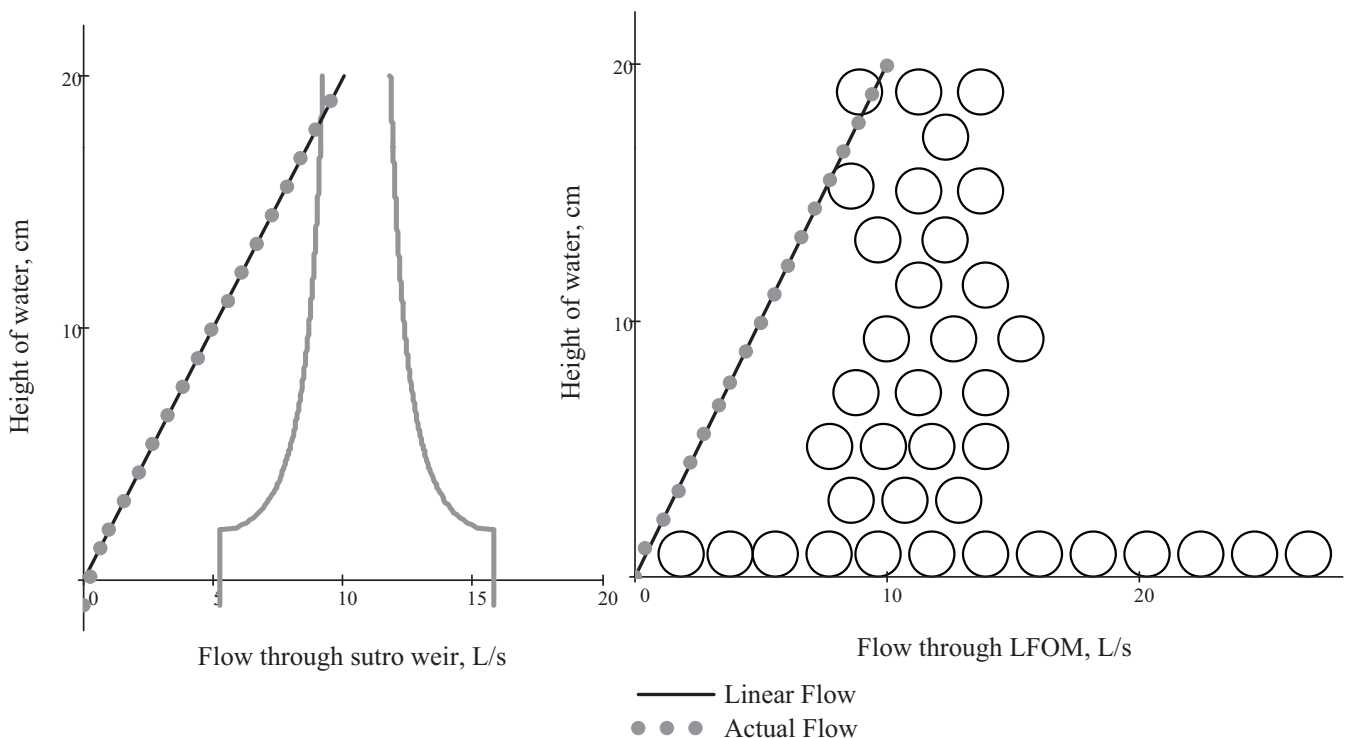


Figure 2: Performance of a) a Sutro weir and b) a LFOM designed to provide a  $10\text{ L/s}$  flow over a vertical distance of  $20\text{ cm}$ . Both images are scaled, with the x-axes representing both  $0 - 20\text{ L/s}$  and  $0 - 20\text{ cm}$ . The Sutro weir equation is only valid when the height of water is above the rectangular portion. Therefore, the equation for flow over a rectangular weir,  $Q_{Rect} = \frac{2}{3}WC_D\sqrt{2g}(H_d + s/3)^{2/3}$ , was used to calculate the flow for the Sutro weir when the height of water is less than  $s$ . The base of the Sutro weir,  $W$ , is  $9.76\text{ cm}$ , the height of the rectangular portion,  $s$ , is  $4\text{ cm}$ . The orifices in the LFOM are  $1.905\text{ cm}$  ( $3/4\text{ in.}$ ) in diameter and the row height,  $B_{Row}$ , is  $2\text{ cm}$ .

247 The LCDC is a semi-automated dosing system that allows the plant operator to set and  
 248 maintain a chemical dose over time-varying plant flow rates in a visually-accessible system.  
 249 Dosing changes are made without requiring calculations.

250 The LCDC uses major head loss in the dosing tube to regulate chemical flow. The linear  
 251 relationship between major head loss and the chemical flow rate is given by the Hagen-  
 252 Poiseuille equation (Equation 17).

$$Q_C = \frac{h_f g \pi D_{Tube}^4}{128 \nu L_{Tube}} \quad (17)$$

253 where  $Q_C$  is the chemical flow rate,  $h_f$  is the major head loss,  $D_{Tube}$  is the inner diameter of  
 254 the dosing tube,  $\nu$  is the kinematic viscosity of the chemical solution,  $g$  is the acceleration due  
 255 to gravity, and  $L_{Tube}$  is the length of the small diameter dosing tube. The Hagen-Poiseuille  
 256 equation assumes that the chemical flow is laminar, viscous and incompressible. The equa-

tion also assumes that the flow passes through a straight tube with a constant circular cross-section that is significantly longer than its diameter. Laminar flow in the dosing tube is indicated by a Reynolds number,  $Re$ , less than 2100 (discussed below). The assumption that major head loss regulates flow requires that minor losses be minimized. Experiments related to minimization of minor losses are discussed below.

A number of constraints are applied to the design of the LCDC to ensure that the simplest functional solution is chosen. The design algorithm calculates several key parameters for all available dosing tube diameters and chooses the design with the minimum number of tubes and maximum allowable tube length. The algorithm steps are as follows:

1. calculate the maximum flow rate through each available dosing tube diameter that keeps error due to minor losses below 10%.
2. calculate the total chemical flow rate that would be required by the treatment system for the maximum chemical dose and the maximum allowable stock concentration.
3. calculate the number of dosing tubes required if the tubes flow at maximum capacity.
4. calculate the length of dosing tube(s) that correspond to each available tube diameter.
5. select the longest dosing tube that is shorter than the maximum tube length allowable based on geometric constraints.
6. select the dosing tube diameter, flow rate, and stock concentration corresponding to the selected tube length.

For the majority of inputs, limiting the effect of minor losses dictates the design. This constraint is addressed by solving a system of equations where  $L_{Tube}$  and the maximum chemical flow rate,  $Q_{MaxError}$ , are both unknown. Rearranging equation 17 gives the mechanical energy loss due to shear on the tube wall or major head loss:

$$h_f = \frac{128\nu L_{Tube} Q_C}{g\pi D_{Tube}^4} \quad (18)$$

where  $h_f$  is the major head loss, which is the lost mechanical energy expressed as a change in elevation. Minor head loss is the mechanical energy loss to deceleration of the fluid caused by changes in the flow geometry and can be calculated by Equation 19.

$$h_e = \frac{8Q_C^2}{g\pi^2 D_{Tube}^4} \sum K \quad (19)$$

where  $\sum K$  is the sum of the minor loss coefficients, all of which use the average velocity in the tube as their reference velocity. The total head loss,  $h_L$ , is the sum of the major and minor losses.

$$h_L = h_f + h_e \quad (20)$$

The maximum departure from the idealized linear relationship between flow and head loss is equal to the minor loss contribution normalized by the total head loss (Equation 21).

$$\Pi_{LinearError} = \frac{h_e}{h_L} \quad (21)$$

288 The maximum flow for a dosing tube will produce an error of  $\Pi_{LinearError}$ , which is limited  
 289 to 10% in the design algorithm. This maximum allowable flow rate,  $Q_{MaxError}$ , based on  
 290 allowable error can be obtained by substituting Equation 19 into Equation 21 and solving  
 291 for  $Q_C$

$$Q_{MaxError} = \frac{\pi}{4} D_{Tube}^2 \sqrt{\frac{2gh_L \Pi_{LinearError}}{\sum K}} \quad (22)$$

292 There is a maximum flow rate for each chemical dosing tube diameter. The array of tube  
 293 diameters is determined by the available tubes and barbed fittings on the market.

294 The flow through the dosing tube must be laminar and this sets an upper bound on the  
 295 tubing diameter that can be used. Equation 22 can be solved for the maximum average  
 296 velocity by dividing by the cross sectional area of the tube.

$$V_{MaxError} = \sqrt{\frac{2gh_L \Pi_{LinearError}}{\sum K}} \quad (23)$$

297 The laminar flow constraint is met when the Reynolds number,  $Re$ , is less than the value  
 298 representing the transition to turbulence,  $Re_{Transition} = 2100$ , and prevents the use of large  
 299 diameter tubes that would also correspond to very long dosing tubes.

$$Re = \frac{VD_{Tube}}{\nu} \quad (24)$$

300 The maximum tubing diameter,  $D_{TubeMax}$  than can be used at the maximum flow rate  
 301 and still maintain laminar flow is obtained by substituting Equation 23 into Equation 24  
 302 and solving for the tubing diameter.

$$D_{TubeMax} = \nu Re_{Transition} \sqrt{\frac{\sum K}{2gh_L \Pi_{LinearError}}} \quad (25)$$

303 The minimum chemical flow rate required by a water treatment plant,  $Q_{Min}$ , given the  
 304 maximum allowable stock concentration,  $C_{StockMax}$ , is

$$Q_{Min} = \frac{Q_{Plant} C_{DoseMax}}{C_{StockMax}} \quad (26)$$

305 where  $C_{DoseMax}$  is the maximum required dose in the plant and  $C_{StockMax}$  is the maximum  
 306 allowable stock concentration. The number of tubes required to deliver that flow rate,  $N_{Tube}$ ,  
 307 for each available tube diameter is calculated and rounded up to the nearest integer.

$$N_{Tube} = \frac{Q_{Min}}{Q_{MaxError}} \quad (27)$$

308 Because the design uses a discrete number of tubes and discrete tube diameters, the  
 309 actual maximum flow through all tubes,  $Q_C$  is calculated for each available tube diameter  
 310 (Equation 28).

$$Q_C = Q_{MaxError} N_{Tube} \quad (28)$$

Table 2: Summary of Design Specifications for a Linear Chemical Dose Controller (LCDC)

Input	Value	Output	Value
$Q_{Plant}$	10 L/s	$D_{Tube}$	3.175 mm (1/8 in)
<i>Tube Diameters</i>	US Standard	$L_{Tube}$	1.03 m
$h_L$	20 cm	$N_{Tube}$	1
$\sum K$	4	$Q_C$	2.3 mL/s
$\Pi_{LinearError}$	0.1	$C_{Stock}$	260 g/L PACl
$C_{StockMax}$	400 g/L		
$C_{DoseMax}$	60 mg/L		
$L_{TubeMax}$	2 m		

311 This algorithm maximizes the flow through each dosing tube to reduce the required length  
 312 of the dosing tubes. If lower flow rates were used, the tubing would need to be made longer  
 313 to achieve the target head loss. The concentration of the chemical stock,  $C_{Stock}$ , is calculated  
 314 for each available tube diameter because of its effect on the chemical viscosity,  $\nu$  (Equation  
 315 29). Variation of coagulant viscosity with concentration was experimentally determined and  
 316 is discussed below.

$$C_{Stock} = \frac{Q_{Plant} C_{DoseMax}}{Q_C} \quad (29)$$

317 The tube lengths that correspond to the available tube diameters are based on the re-  
 318 lationship between the maximum error and major and total losses by combining Equations  
 319 18, 19, 20, 21, and 22 and solving for the tube length.

$$L_{Tube} = (1 - \Pi_{LinearError}) \frac{D_{Tube}^2}{64\nu} \sqrt{\frac{2gh_L \sum K}{\Pi_{LinearError}}} \quad (30)$$

320 The length of the tube increases with the square of the tubing diameter. This creates a  
 321 practical upper limit on the tubing diameter that can be used while maintaining a length of  
 322 tubing that can be accommodated easily in the water treatment plant. The optimal design  
 323 is chosen by selecting the tube diameter, stock concentration, and chemical flow rate that  
 324 correspond to the longest tube that does not exceed the maximum length specified by the  
 325 user.

326 The parameters noted above are summarized in Table 2 for an example plant with a  
 327 maximum flow of 10 L/s and are implemented in a design algorithm to select a dosing tube  
 328 diameter and length, chemical stock tank concentration, and number of dosing tubes. The  
 329 resulting designs for different plant flow rates are shown in Figure 4. Custom designs for  
 330 chemical dose controllers may be obtained from the AguaClara Design Tool ([aguaclara.cornell.edu/design](http://aguaclara.cornell.edu/design)).  
 331

## 332 Experimental Methods

### 333 Determination of minor head loss coefficient

334 If the major losses dominate minor losses, the linear relationship between the chemical flow  
335 rate and the major head loss described by Equation 17 would be maintained. Minor head  
336 losses caused by flow expansions and contractions as well as tube curvature are proportional  
337 to the square of the chemical flow rate. The magnitudes of the minor head losses were  
338 modeled in tandem with experimental analysis to minimize their sources. The total head  
339 loss through the system ( $h_L$ ) is the sum of the major ( $h_f$ ) and minor ( $h_e$ ) head losses.  
340 Therefore, the total head loss through the system can be represented as:

$$h_L = \frac{128\nu L_{Tube}}{g\pi D_{Tube}^4} Q_C + \frac{8 \sum K}{g\pi^2 D_{Tube}^4} Q_C^2 \quad (31)$$

341 There are two terms in Equation 31, one with a linear relationship between head loss  
342 and chemical flow rate, the other non-linear. The minor head loss coefficient can only be  
343 roughly estimated by summing standard values for each change in flow path, but should be  
344 experimentally determined. The minor head loss coefficient for the tested tubing configu-  
345 ration was determined from the array of observed flow rate data and total head loss values  
346 using Equation 31. Once  $\sum K$  is determined for a particular tubing configuration, it can be  
347 used to design similar systems for all tube diameters and lengths.

### 348 LCDC Prototype Calibration and Testing

349 LCDC performance tests were conducted in the laboratory using a stationary test stand  
350 to simulate changes in plant flow rate. The end of the lever arm that would normally  
351 connect to the float was adjusted by inserting a metal pin into holes at specified elevations  
352 in the test stand. By setting the driving head directly, deviations from the expected flow  
353 rates were attributed to minor losses only. With the slider at the maximum dose, the flow  
354 rates through the small diameter dosing tubes and the large diameter connector tubes were  
355 measured for tube lengths of 1.32 m to 2.56 m and driving head 0–20 cm in 4 cm increments.  
356 At each position, three 60 second flow tests were performed and the mean was compared to  
357 the expected flow rates. Field tests must ultimately verify that the the maximum desired  
358 coagulant flow rate can be achieved.

359 Calibration of the LCDC system in the field requires adjusting the length of the chain  
360 that connects the float to the lever arm to ensure that the lever arm is horizontal at zero plant  
361 flow with the slider at maximum chemical dose. Next, with the lever arm still horizontal, the  
362 constant head tank must be raised or lowered so that there is no flow through the dosing tube  
363 until the lever arm float is raised. The plant flow should then be set to maximum and the  
364 chemical flow rate measured. If the flow rate is different than predicted by the algorithm,  
365 the length of the dosing tube(s) should be adjusted to achieve less than 5% error at the  
366 maximum chemical flow rate (maximum dose and maximum plant flow rate). Guidelines  
367 for calibration suggest starting with a dosing tube 10% longer than calculated by the design  
368 algorithm and then shortening it in 2 cm increments until a satisfactory agreement wit the  
369 maximum flow is obtained.

## 370 Results

### 371 Minimizing the Minor Loss Coefficient

372 Minor losses in the LCDC system cause the flow rate to become increasingly nonlinear with  
373 respect to head loss, increasing the errors in dosing. Since minor losses are caused by changes  
374 in the flow geometry, several dosing tube configurations were tested to quantify their impact  
375 on the sum of the minor loss coefficients (Figure 5).

376 Tube curvature was found to be a significant source of minor losses. Perfectly straight  
377 tubing had the lowest  $\sum K$  value (2.74). The highest measured loss coefficient (10.36) was  
378 observed when the tubing was allowed to drape freely. The optimal tube configuration  
379 that allowed the needed flexibility was obtained by reducing minor losses associated with  
380 curved tubing and connectors. The curved tubing was straightened by attaching a weight  
381 to the dosing tube at the low point between the constant head tank and the drop tube,  
382 which decreased  $\sum K$  to 5.79. The connector losses were also significant and the minor  
383 loss coefficient present with straightened tubing was reduced to  $\sum K = 3.13$  by providing a  
384  $0.952\text{ cm}$  ( $3/8\text{ in}$ ) connector tube. The connector tube decreases the flow velocity and thus  
385 reduces the minor losses in the fittings and at the point where the flexible tube connects  
386 to the drop tube. The length of the connector tube can be adjusted without affecting the  
387 accuracy of the dosing system.

### 388 LCDC Performance Testing

389 A series of flow tests were carried out for a  $1.42\text{ m}$  dosing tube with a weight and a  $0.952\text{ cm}$   
390 ( $3/8\text{ in}$ ) inner diameter connector tube as described previously. The results are displayed  
391 in Figure 6; also displayed are the flow rates calculated using the Hagen-Poiseuille equation  
392 for major losses (Equation 17). By fitting the observed flow rates to the total head loss  
393 equation (which includes both major and minor losses) (Equation 31) and using a least  
394 squares regression, the minor loss coefficient,  $\sum K$ , was estimated to be 3.13.

### 395 Error caused by slider mass

396 An additional source of error in dose is caused by movement of the slider along the lever  
397 arm. Due to the mass of the slider and drop tube on the slider side of the lever arm, there is  
398 a variable moment about the pivot point as the slider is moved, which causes a change in the  
399 force acting on the float. The change in height of the float when the slider is moved will cause  
400 an error in chemical dose. The error resulting from a change in submergence of the float is  
401 directly dependent on the total mass of the slider assembly. The vertical displacement of the  
402 float,  $\Delta h$ , as a function of float diameter,  $D_{Float}$ , is calculated in Equation 32.

$$\Delta h = \frac{4M_{Slider}}{\pi D_{Float}^2 \rho_{Water}} \quad (32)$$

403 The lever is leveled at zero plant flow with the slider at maximum chemical dose. Because  
404 flow through the dosing tube is linearly proportional to height, the maximum displacement  
405 error is  $\Delta h/H_{LFOM}$ . The maximum allowable error due to changing submergence of the float

406 is given by  $\Pi_{FloatError}$ , and is set equal to 5% for the calculations presented in this paper.  
 407 The minimum float diameter that adheres to this constraint,  $D_{MinFloat}$ , is given by Equation  
 408 33.

$$D_{MinFloat} = \sqrt{\frac{4M_{Slider}}{\pi\rho_{Water} \cdot \Pi_{FloatError} h_L}} \quad (33)$$

409 With a slider assembly mass,  $M_{Slider}$ , of 120 g,  $D_{MinFloat}$  for the experimental prototype  
 410 was 12.36 cm (4.86 in); a float diameter of 15 cm (6 in) was used. The prototype has a  
 411 maximum float displacement of 0.658 cm. This error is eliminated by calibration at the  
 412 maximum chemical dose and then grows to 3.3% for smaller chemical dosages. Moving the  
 413 slider away from the maximum dose position decreases its moment and decreases the dose  
 414 which counteracts the increased dose due to minor loss error in the mid dose range. The  
 415 area of the float at the air-water interface can be increased by using a 20 cm (8 in) diameter  
 416 float to distribute the volume of displaced water over a larger area, and reduce the maximum  
 417 displacement error to 1.9%. For plant flow rates large enough to warrant multiple dosing  
 418 tubes or a larger drop tube, the mass of the slider assembly will increase the dosing error,  
 419 motivating the switch to a larger float diameter.

## 420 Coagulant Viscosity

421 The viscosity of the chemical solution has a considerable impact on the design and perfor-  
 422 mance of the LCDC. Little information is available regarding the viscosity of high concentra-  
 423 tion coagulant solutions. Therefore, experiments were performed with a Vibro Viscometer  
 424 to directly measure the kinematic viscosity of alum and PACl solutions with concentrations  
 425 ranging from 10 g/L to 600 g/L of alum and PACl at 20°C (Figure 7). To better mimic  
 426 coagulants used in water treatment practice, industry grade polyaluminum chloride (PACl),  
 427 (Amuco, Inc.), and technical grade aluminum sulfate,  $Al_2(SO_4)_3 \cdot 14.3H_2O$ , (PTI Process  
 428 Chemicals) were used as coagulants for all experiments. Each coagulant was diluted with  
 429 distilled water to make the stock solutions.

430 Kinematic viscosity must be taken into account when predicting chemical flow rates  
 431 through the LCDC system. Fits to the experimentally observed relationships were used in  
 432 the LCDC design algorithms to properly estimate the expected chemical flow through the  
 433 small diameter dosing tube (Equations 34 and 35).

$$\nu_{Alum} = \nu_{Water} \left( 1 + 4.255 \times 10^{-6} C_{Alum}^{2.289} \right) \quad (34)$$

$$\nu_{PACl} = \nu_{Water} \left( 1 + 2.383 \times 10^{-5} C_{PACl}^{1.893} \right) \quad (35)$$

434 where  $\nu_{Water}$  is the viscosity of water at 20°C, 1 mm<sup>2</sup>/s,  $C_{Alum}$  is the alum concentration  
 435 in g/L alum, and  $C_{PACl}$  is the PACl concentration in g/L PACl. The curve fits for Alum  
 436 and PACl have a sample size,  $N$ , of 13 and  $R_{Alum}^2 = 0.99$  and  $R_{PACl}^2 = 0.97$ . The reader  
 437 is cautioned that these relationships are for industry and technical grade chemicals, and  
 438 that other suppliers may provide different compositions. Preliminary tests suggested that  
 439 viscosity did not vary significantly from  $\nu_{Water}$  for calcium hypochlorite. Accurate viscosity  
 440 data is required before designing the LCDC for use with other chemicals.

## 441 Conclusions

442 The linear chemical dose controller and linear flow orifice meter work in concert to provide a  
443 gravity-powered semi-automated chemical dosing system whose function is explained entirely  
444 by basic hydraulics, and can be easily fabricated. Through many tests and prototypes, we  
445 have converged on a dosing system design that minimizes deviation from the desired linear  
446 relationship. Experiments show that use of straight dosing tube segments and connector tube  
447 can minimize minor losses. The additional error in dosing created by the variable moment  
448 that the slider assembly causes about the pivot point can be minimized by a large diameter  
449 float and small mass slider assembly design. Careful component selection and fabrication can  
450 ensure that the system will function properly with any chemical solution for a wide range  
451 of chemical and plant flow rates (Appendices A and B). The dosing system is versatile, and  
452 was designed with the end-user in mind. The design equations have been incorporated into  
453 a design algorithm that takes as input the target plant flow rate and outputs all necessary  
454 design specifications (available at [aguaclara.cornell.edu/design](http://aguaclara.cornell.edu/design)). Variation of stock chemical  
455 viscosity is considered in the design calculations. The coupled LCDC and LFOM have been  
456 tested in six gravity-powered municipal scale drinking water treatment plants designed by  
457 the AguaClara Program at Cornell University and built in Honduras. Operator feedback is  
458 positive and the systems continue to perform as designed.

## 459 Acknowledgments

460 The research described in this paper was funded by the Sanjuan Foundation. This project  
461 was supported by a number of people at Cornell University, including Paul Charles, Timo-  
462 thy Brock, Alexander Krolick, Michael Adelman, and Dale Johnson. Special thanks go to  
463 Matthew Higgins, Jordanna Kendrot, and David Railsback for their work on early prototypes  
464 of the LFOM and LCDC.

## 465 References

- 466 Brikke, F., Bredero, M., 2003. Linking technology choice with operation and maintenance in  
467 the context of community water supply and sanitation: A reference document for planners  
468 and project staff. Tech. rep., World Health Organization and IRC Water and Sanitation  
469 Centre.
- 470 Franz, D. D., Melching, C. S., 1997. Full equations utilities (fequtl) model for the approxima-  
471 tion of hydraulic characteristics of open channels and control structures during unsteady  
472 flow. Water Resources Investigations Report 97-4037, U.S. Geological Survey.
- 473 Thandaveswara, B. S., 2012. Proportional weirs. Tech. rep., Indian Institute of Technology  
474 Madras.
- 475 World Health Organization, 2011. Fact sheets on environmental sanitation: fact sheet 2.22-  
476 dosing hypochlorite solutions. Tech. rep.



## 477 Appendices

### 478 Appendix A: Fabrication and Component Selection

479 In adherence to the sustainable design constraints stated above, the LCDC should, to the  
480 extent possible, be made of locally available materials. Therefore, it is important to define  
481 the characteristics of each component that are necessary to good performance vs. those  
482 which are incidental. The system components are designated in Figures 3 and 8 and their  
483 necessary characteristics are as follow:

- 484 • The **constant head tank** should have a wide mouth to allow operator access and a  
485 diameter that fits the float valve. It should have a cover to prevent debris from entering  
486 the chemical solution and one or more small holes in the cover to ensure atmospheric  
487 pressure inside. The through-wall bulkhead fittings that connect the dosing tubes to  
488 the constant head tank should be barbed and one size larger than dictated by the  
489 diameter of the dosing tube to minimize minor losses due to contractions/expansions.  
490 A rubber o-ring prevents leaking at the bulkhead connections.
- 491 • The **float valve** in the constant head tank (CHT) is the only component that may  
492 not be locally sourced in all countries; it is manufactured by Kerick Valves, Inc. and  
493 the size used is set by the diameter of the orifice inside the float valve. The orifice  
494 diameter needed for the maximum chemical flow rate can be calculated by the orifice  
495 equation ( $Q = \Pi_{vc} \frac{\pi}{4} D^2 \sqrt{2gh}$  ).
- 496 • The **dosing tube** must be kept taut by a weight of approximately 20 g to reduce minor  
497 losses due to curvature to maintain straight sections of tubing.
- 498 • The dosing tube, attaches to a larger (0.25 – 0.5 in) inner diameter “**connector**”  
499 **tube** with a reducing barbed fitting. Experimental results revealed that attaching the  
500 connector tube to the drop tubes rather than attaching the dosing tube directly reduced  
501 the minor loss coefficient by 46% (See Figure 5). Therefore, the large diameter tube  
502 should be used even in plants where additional length is not required. The length of  
503 the connector tube is arbitrary and allows the placement of the constant head tank to  
504 be more flexible. The connector tube attaches to the drop tube with an NPT-threaded  
505 barbed fitting that is also one size larger than the tube diameter.
- 506 • The **drop tube** should be transparent to allow the operator to visually confirm chem-  
507 ical flow. The drop tube must be of sufficient length that the bottom of the drop tube  
508 is below the lowest water level in the flocculator (zero plant flow). This prevents air  
509 from entering the flexible tubing that connects the drop tube to the rapid mix; air  
510 in the tubing would create an additional head loss in the flexible tubing which causes  
511 intermittent chemical flow to the plant.
- 512 • The **lever arm** should be a three foot long aluminum bar, approximately 2 in wide  
513 to provide space for the dosing scale below the slider and to prevent the slider from  
514 obscuring reading of the dose. The lever arm should be mounted to the side of the  
515 entrance tank at the pivot point.

Table 3: Detailed list of components for the LCDC. This listing is for a LCDC designed for a 10 L/s water treatment plant. Depending on the plant capacity, different quantities or sizes may be required.


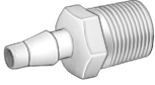








- 516 • The **scale** may be printed on a sticker attached to the lever arm, or stamped directly  
 517 onto the aluminum lever arm. The scale is to be defined in  $\frac{mg}{L}$  of the coagulant or as  
 518 a percentage of the maximum dose.
- 519 • The **slider** should also be aluminum, with one threaded hole for a small screw that  
 520 acts as a locking mechanism, and another similar screw that holds the drop tube. This  
 521 connection should be loose, allowing free rotation of the drop tube, which should be  
 522 vertical at all times. The slider assembly (slider, screws, drop tube, barbed fitting)  
 523 should be as light as possible because it creates a variable moment about the central  
 524 pivot that is compensated for by a shift in the height of the float (see *Error caused by*  
 525 *mass of the slider* above). To accommodate large flow plants where multiple dosing  
 526 tubes are needed, a “T”-shaped slider assembly can be used. The “T” is made of the  
 527 same clear PVC as the drop tubes, and each of the barbed fittings is located along  
 528 a horizontal bar that adjusts to be level with the ground as the lever arm moves. In  
 529 the case of multiple tubes, all tubes supply the desired chemical doses simultaneously,  
 530 allowing the LCDC to dose plants with high flow rates. A counterweight can be used  
 531 to maintain tension in the chain connecting the float to the lever arm if the variable  
 532 moment caused by the slider is insufficient (See Figure 8).
- 533 • The **float** should be as wide and short as possible. The float should not touch the  
 534 bottom of the entrance tank at zero plant flow and should be water tight. The mass of  
 535 the float should be high compared to the mass of the slider assembly. The float must  
 536 have a center of gravity that is below the center of buoyancy to provide stability.






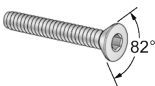


537 A list of parts used in the LCDC prototype is included in the Supplemental Materials section  
 538 (Table 3).




539 While chemical compatibility between the aluminum and PVC components and coagu-  
 540 lant and chlorine solutions will protect the LCDC from degradation over time, occasional  
 541 maintenance is required. If calcium hypochlorite is used as a disinfectant, calcium carbon-  
 542 ate precipitate forms when the chlorine solution comes in contact with atmospheric carbon  
 543 dioxide, and the upper, open end of the drop tubes are likely to develop significant calcium  
 544 carbonate precipitate. Periodically, this will need to be removed or dissolved with vinegar  
 545 so it does not interfere with the chemical flow.

## 546 Appendix B: Components List

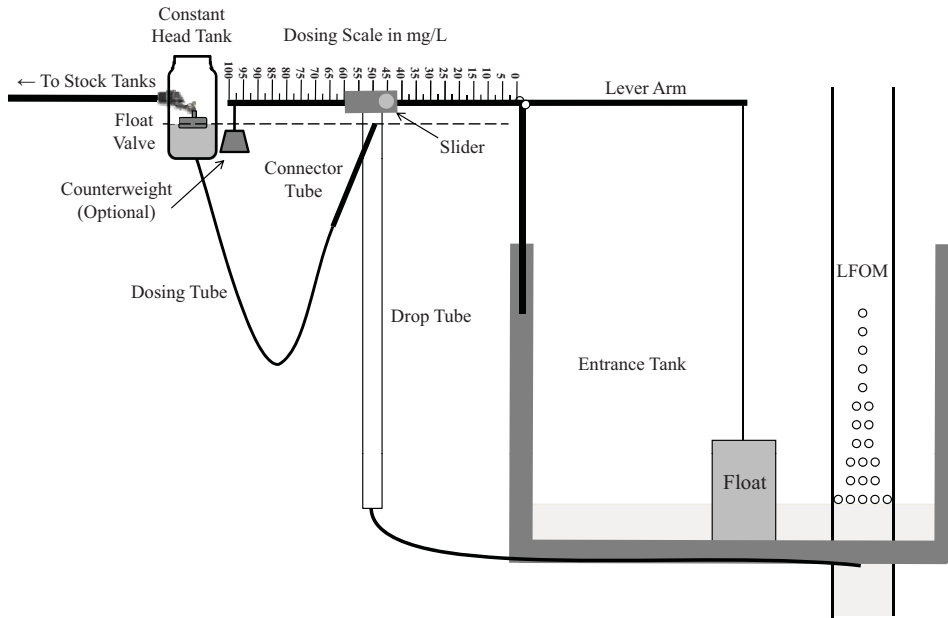
Part Name	Picture	Description and Explanation
-----------	---------	-----------------------------

Barbed Fitting for Constant Head Tank		Durable nylon single-barbed tube fitting through-wall adapter for connecting the dosing tube to the CHT.
Barbed Fittings for Drop Tubes		Allows the chemical/coagulant to enter the drop tube from the 0.952 cm (3/8 in) inner diameter connector tube.
Reducing Barbed Fittings		Reducing barbed fitting that goes from 0.317 cm (1/8 in) inner diameter dosing tube to 0.952 cm (3/8 in) inner diameter connector tube.
PVC Drop Tubes		Clear plastic so that plant operator can observe flow. Should be 1.22 cm (1/2 in) in diameter to keep as lightweight as possible while ensuring free fall of the chemical solution.
PVC Tubes for Counterweight		A short (5 cm) section of PVC pipe can be used as the optional counterweight.
Large Diameter Connector Tubing		Clear plastic tubing with 0.952 cm (3/8 in) inner diameter to be used as a connector to the drop tube.
Small Diameter Dosing Tubing		Attached to the base of the CHT and the connector tube via a reducing barbed fitting. Clear 0.317 cm (1/8 in) inner diameter. Length specified by the algorithm.
PVC Tee		1.24 cm (1/2 in) PVC tee. Used for a T-shaped slider assembly when the algorithm recommends more than one dosing tube for higher flow systems.
PVC Pipe Cap		Schedule 40 white PVC pipe cap attached to the ends of the "T" and to the bottom of the drop tubes.
Turnbuckle		Connects the float chain to the lever-arm apparatus. Allows for adjustment during calibration.

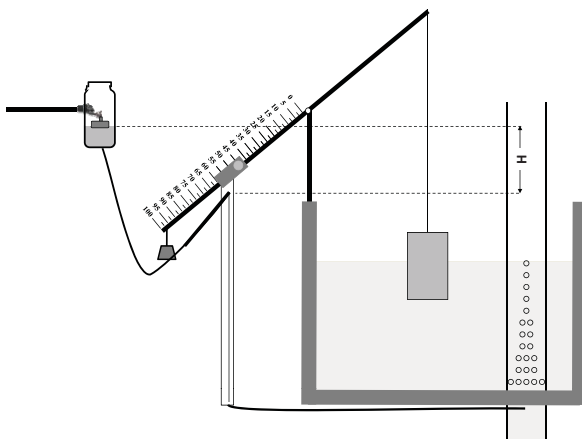
Constant Head Tank		Translucent plastic jar (2 L), 14.92 cm base diameter, 15.88 cm height with a hole drilled in the bottom center for the through-wall barbed fitting. The cover prevents contamination of the chemical by particles in the air, but does not make the container air-tight. Small drilled holes can be used to allow air flow.
Lever Arm		Aluminum, 0.914 m (3 ft) in length, 5 cm (2 in) in width, and 0.635 cm (1/4 in) in thickness.
Slider		Corrosion resistant aluminum, u-channel, 0.317 cm (1/8 in) thick, 1.27 cm (1/2 in) base, 1.905 cm (3/4 in) legs, 10.16 cm (2 in) in length. Attached to the top of the lever arm to vary the coagulant dose.
Aluminum shaft collar		0.952 cm (3/8 in) bore, 1.905 cm (3/4 in) outer diameter, 0.952 cm (3/8 in) width; aluminum shaft collars are secured on either side of each of the lever arms to prevent the lever arms from shifting laterally along the shaft
Hex nut		For use between the drop tube and the slider. Permits the drop tube to swing freely.
Screws		1.27 cm (1/2 in) 10-32 screws. One for the slider locking mechanism, one to hang the drop tube
Kerick Float Valve		Attached to the side of the constant head tank, and it keeps the water level constant inside the CHT.
Square head plug		15.24 cm (6 in) PVC threaded square head plug for the top of the float. Water tight but removable to allow weight to be added to the float

PVC cap		15.24 <i>cm</i> (6 <i>in</i> ) unthreaded PVC cap for the bottom of the float
Threaded adapter		15.24 <i>cm</i> (6 <i>in</i> ) threaded adapter to receive the square head plug and convert to unthreaded pipe
PVC pipe		15.24 <i>cm</i> (6 <i>in</i> ) pipe is needed to connect the adapter to the PVC cap. Use no more than is necessary for this purpose.

a)



b)



c)

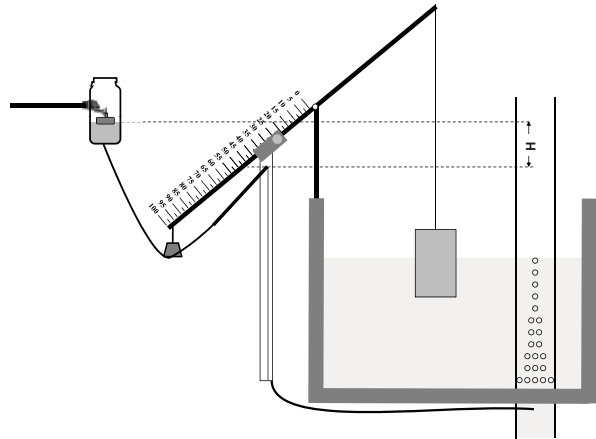


Figure 3: Linear chemical dose controller schematic under conditions of: a) no flow, b) maximum flow, and c) maximum flow with a lower chemical dose.

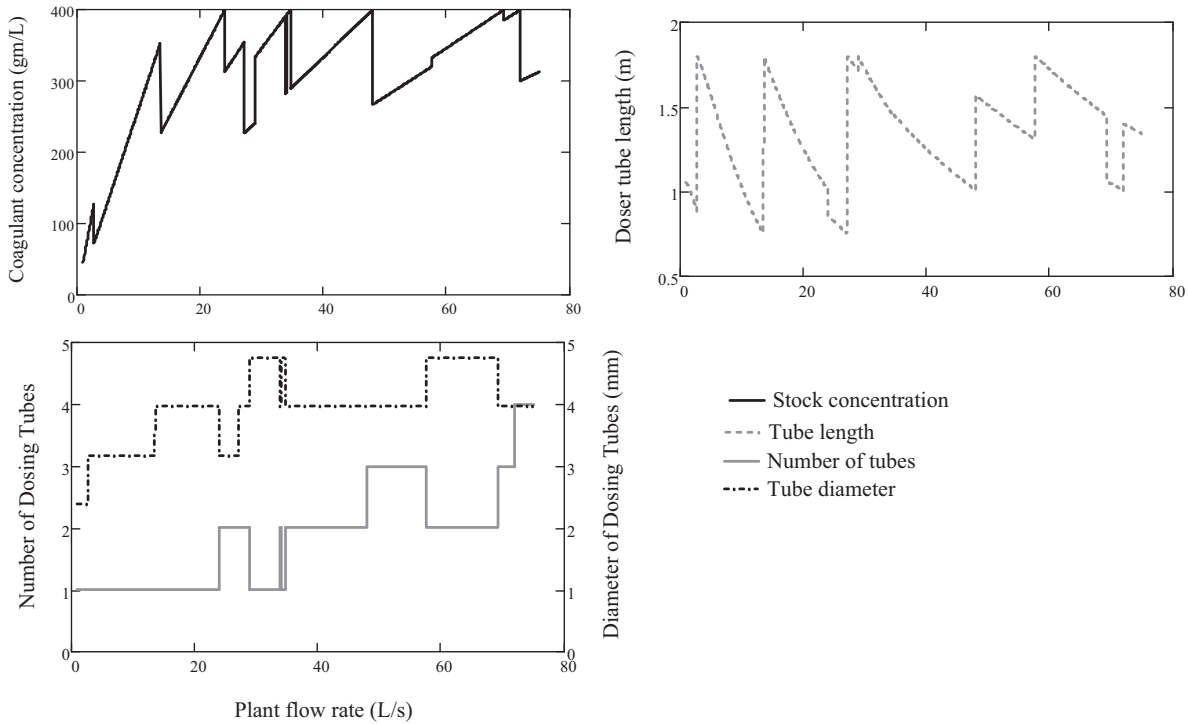


Figure 4: LCDC design algorithm results for plant flow rates 1 – 75  $L/s$ . As the flow rate changes, the dominating constraint may change causing the values given by the algorithm to fluctuate. The discontinuities shown are caused by the discrete sizes of tubing and the requirement of an integer number of tubes. For example at approximately 3  $L/s$  the algorithm changes the specified diameter of the dosing tube from 2.38 mm ( $3/32$  inch) to 3.175 mm ( $1/8$  inch) and the doser tube length and coagulant concentrations must both change to maintain constant dose.

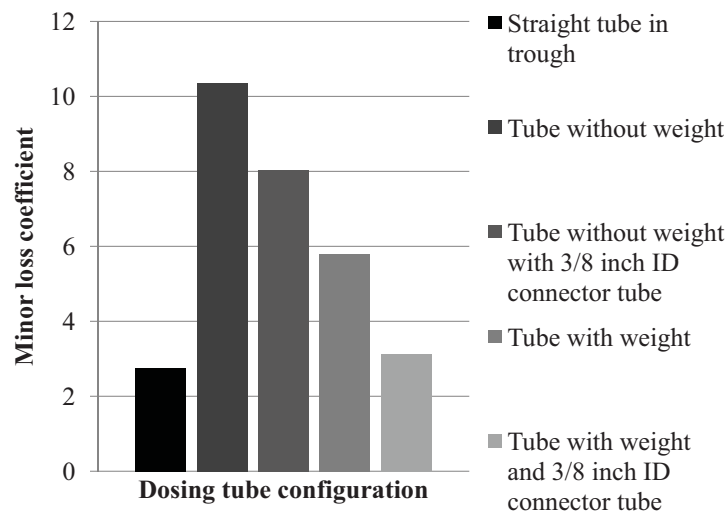


Figure 5: Minor loss coefficients for alternative tubing configurations. Values are an average of three trials for a 1.42  $m$  dosing tube over a range of head losses (0 – 20 cm).

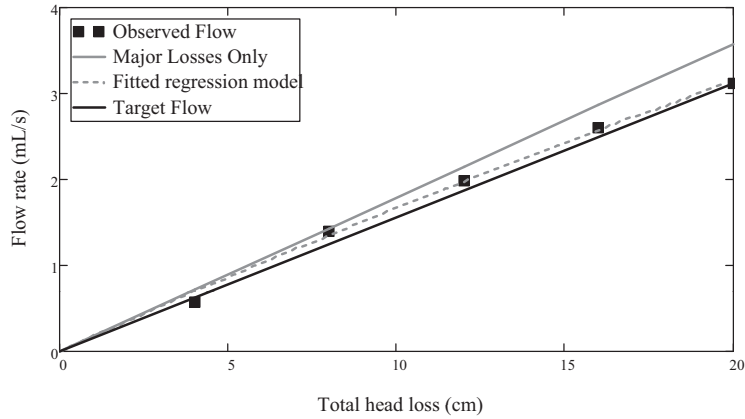


Figure 6: Performance test results from a  $0.317\text{ cm}$  ( $1/8\text{ in}$ )  $1.42\text{ m}$  dosing tube with a weight and a  $0.952\text{ cm}$  ( $3/8\text{ in}$ ) connector tube using tap water with  $\nu_{Water} = 1\text{ mm}^2/\text{s}$ . A least-squares regression used the initial observed flow rates to fit a minor loss coefficient,  $\sum K$ , of 3.13. Field calibration occurs at zero flow and at maximum flow where the deviation from flow expectations based solely on major losses is greatest. Thus, the calibration procedure compensates for minor losses at the maximum flow. Minor losses cause some deviation from the linear relation between the two calibration points but this error is less than 10%

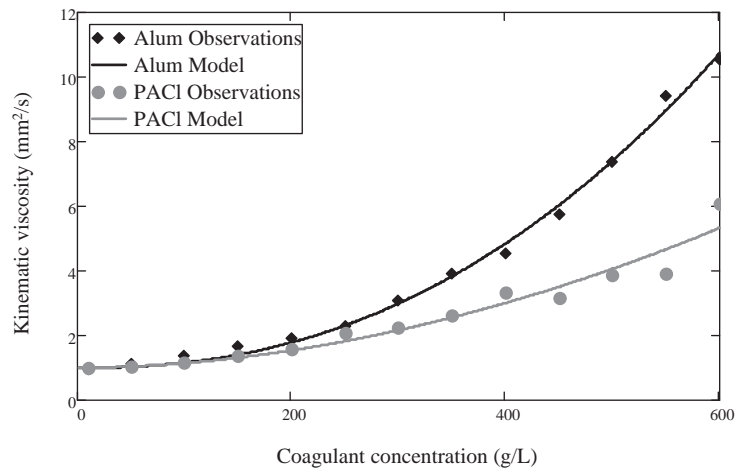


Figure 7: Experimentally determined kinematic viscosities of alum and PACl solutions for use as chemical stock concentrations.



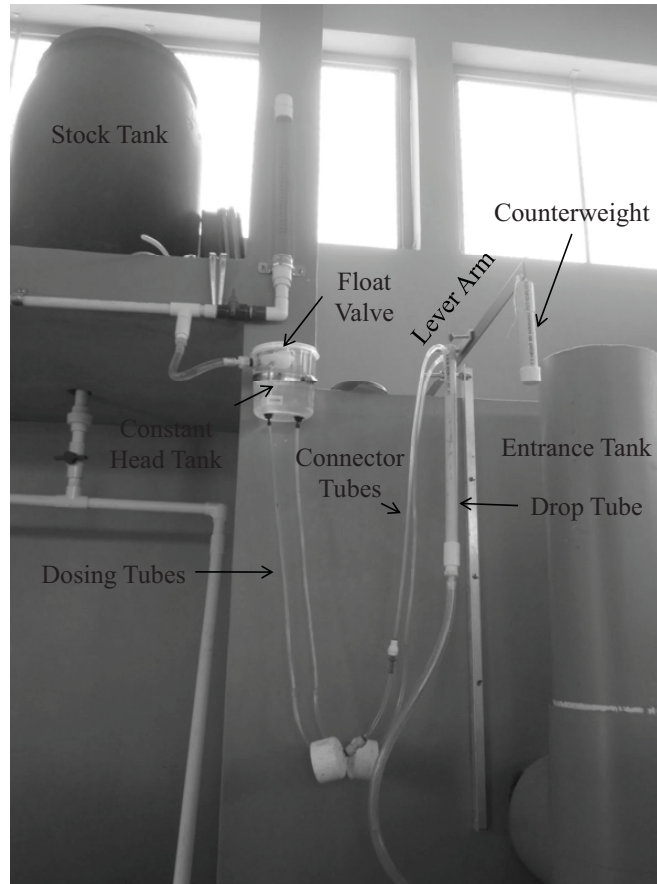


Figure 8: LCD in operation at the Alauca municipal water treatment plant in Alauca, Honduras. Plant flow rate is  $12 L/s$ .